



King Saud University
Journal of Saudi Chemical Society

www.ksu.edu.sa
www.sciencedirect.com



ORIGINAL ARTICLE

Spectroscopic and molecular modeling studies of N-(4-(3-methyl-3-phenylcyclobutyl)-3-phenylthiazole-2(3H)-ylidene)aniline by using experimental and density functional methods

Fatih Şen ^{a,*}, Öner Ekici ^b, Muharrem Dinçer ^c, Alaaddin Cukurovali ^b

^a Kilis 7 Aralık University, Vocational High School of Health Services, Department of Opticianry, 79000 Kilis, Turkey

^b Firat University, Sciences Faculty, Department of Chemistry, 23119 Elazığ, Turkey

^c Ondokuz Mayıs University, Arts and Sciences Faculty, Department of Physics, 55139 Samsun, Turkey

Received 10 February 2015; revised 8 April 2015; accepted 6 May 2015

KEYWORDS

Cyclobutane;
Thiazole;
Density functional theory (DFT);
Non-linear optical effects;
Frontier molecular orbital analysis (FMO)

Abstract In the present study, a combined experimental and computational study on molecular structure and spectroscopic characterization on the title compound has been reported. The crystal was synthesized and its molecular structure brought to light by X-ray single crystal structure determination. The spectroscopic properties of the compound were examined by FT-IR and NMR (¹H and ¹³C) techniques. FT-IR spectra of the target compound in solid state were observed in the region 4000–400 cm⁻¹. The ¹H and ¹³C NMR spectra were recorded in CDCl₃ solution. The molecular geometries were those obtained from the X-ray structure determination optimized using the density functional theory (DFT/B3LYP) method with the 6-31G(d, p) and 6-31G+(d, p) basis set in ground state. From the optimized geometry of the molecule, geometric parameters (bond lengths, bond angles and torsion angles), vibrational assignments and chemical shifts of the title compound have been calculated theoretically and compared with those of experimental data. Besides, molecular electrostatic potential (MEP), frontier molecular orbitals (FMOs), Mulliken population analysis, Thermodynamic properties and non-linear optical (NLO) properties of the title molecule were investigated by theoretical calculations.

© 2015 The Authors. Production and hosting by Elsevier B.V. on behalf of King Saud University. This is an open access article under the CC BY-NC-ND license (<http://creativecommons.org/licenses/by-nc-nd/4.0/>).

* Corresponding author.

E-mail address: fatihsen55@gmail.com (F. Şen).

Peer review under responsibility of King Saud University.



Production and hosting by Elsevier

1. Introduction

In recent years, thiazole and its derivatives have gained importance with biological and pharmacological activities such as anti-inflammatory [1,2], anticonvulsant [3,4], antifungal [5,6], antitumor [7,8], antitubercular [9,10], antimicrobial [11–13] and analgesic [14]. In relation to these effects, thiazole ring is

<http://dx.doi.org/10.1016/j.jscs.2015.05.004>

1319-6103 © 2015 The Authors. Production and hosting by Elsevier B.V. on behalf of King Saud University.

This is an open access article under the CC BY-NC-ND license (<http://creativecommons.org/licenses/by-nc-nd/4.0/>).

Please cite this article in press as: F. Şen et al., Spectroscopic and molecular modeling studies of N-(4-(3-methyl-3-phenylcyclobutyl)-3-phenylthiazole-2(3H)-ylidene)aniline by using experimental and density functional methods, Journal of Saudi Chemical Society (2015), <http://dx.doi.org/10.1016/j.jscs.2015.05.004>

used in the application of drug development for the treatment of allergies [15,16], hypertension [17], inflammation [18], bacterial [19], HIV infection [20], antioxidant [21], tubercular [22], hypnotics [23] and recently for the treatment of pain [24]. As a consequence of the unique three-dimensional disposition of substituents and torsional ring strain driven by high reactivity, cyclobutanes have received considerable attention of medicinal and synthetic chemists as drug scaffolds and/or synthetic intermediates in routes targeted at medicinally useful substances [25,26]. Cyclobutane itself is of no commercial or biological significance, but more complex derivatives are important in biology and biotechnology [27]. It is well known that 3-Substituted cyclobutane carboxylic acid derivatives exhibit anti-inflammatory and anti-depressant activity [28]. With the effects given above, the compounds containing thiazole and cyclobutane have been seen to be important. The title compound is a novel compound firstly synthesized in our laboratories by us.

The purpose of this work is to investigate the title compound, both experimentally and theoretically. Literature survey reveals that to the best of our knowledge, the results based on X-ray diffraction, spectral studies and quantum chemical calculations on compounds have no reports. In this study, we present the results of a detailed investigation of the synthesis and structural characterization of the title compound using single crystal X-ray diffraction, IR-NMR spectroscopy and quantum chemical methods.

2. Experimental and theoretical methods

2.1. Synthesis and characterization

To a solution of 1,3-diphenylthiourea (2.2831 g, 10 mmol) in 20 mL of absolute ethanol a solution of 2-chloro-1-(3-methyl-3-phenylcyclobutyl)ethanone (2.2271 g, 10 mmol) in 10 mL of absolute ethanol was added. After the addition of the α -haloketone, the temperature was raised to 323–328 K and kept at this temperature for 2 h (IR). The solution was cooled to room temperature and then made alkaline with an aqueous solution of NH_3 (5%), and off white precipitate separated by suction, washed with aqueous NH_3 solution several times and dried in air. Suitable single crystals for crystal structure determination were obtained by slow evaporation of its ethanol solution. Yield: 87%, melting point: 462 K (Scheme 1).

2.2. General remarks

All chemicals were of reagent grade and used as commercially purchased without further purification. Melting point was determined by Gallenkamp melting point apparatus. The IR spectrum of the title compound was recorded in the range of 4000–400 cm^{-1} using a Mattson 1000 FT-IR spectrometer

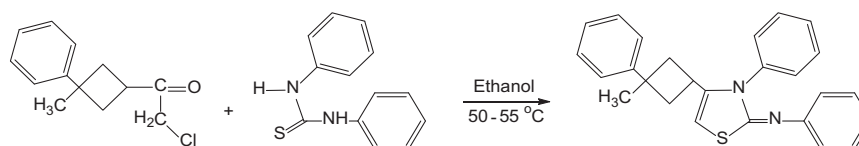
with KBr pellets. The ^1H and ^{13}C nuclear magnetic resonance (NMR) spectra were recorded on a Varian-Mercury-Plus 400 MHz spectrometer using TMS as internal standard and CDCl_3 (chloroform) as solvent.

2.3. Crystal structures determination and refinement

A suitable sample of size $0.650 \times 0.293 \times 0.080$ mm was selected for the crystallographic study. All diffraction measurements were performed at room temperature (296 K) using graphite monochromated $\text{Mo K}\alpha$ ($\lambda = 0.71073 \text{ \AA}$) radiation and an STOE IPDS 2 diffractometer. A total of 20,944 reflections with [$1.2^\circ < \theta < 25.7^\circ$] were collected in the rotation mode and cell parameters were determined using X-Area software [29]. Absorption correction ($\mu = 0.17 \text{ mm}^{-1}$) was achieved by the integration method via X-RED software [29]. The structure was solved by direct methods using SHELXS-97 [30]. All non-hydrogen atoms were refined anisotropically by the full-matrix least squares procedure based on F^2 using SHELXL-97 [31]. All H atoms were positioned geometrically and treated using a riding model, fixing the bond lengths at

Table 1 Crystal data and structure refinement parameters for the title compound.

CCDC deposition No.	1006348
Chemical formula	$\text{C}_{26}\text{H}_{24}\text{N}_2\text{S}$
Formula weight	396.55
Temperature (K)	296
Wavelength (\AA)	0.71073
Crystal system	Orthorhombic
Space group	Pca_2_1
<i>Unit cell parameters</i>	
$a \neq b \neq c$ (\AA)	34.7637 (19), 5.9235 (2), 10.4336 (4)
$\alpha = \gamma = \beta$ ($^\circ$)	90
Volume (\AA^3)	2148.52 (16)
Z	4
Calculated density (Mg/m^3)	1.226
μ (mm^{-1})	0.17
F_{000}	840
Crystal size (mm)	$0.650 \times 0.293 \times 0.080$
$h_{\text{min}}, h_{\text{max}}$	–42, 41
$k_{\text{min}}, k_{\text{max}}$	–7, 7
$l_{\text{min}}, l_{\text{max}}$	–12, 12
$\theta_{\text{max}}, \theta_{\text{min}}$ ($^\circ$)	25.7, 1.2
Measured reflections	20,944
Independent reflections	4029
Refinement method	Full-matrix least-squares on F^2
Goof = S	0.92
$R[F^2 > 2\sigma(F^2)]$	0.045
$wR(F^2)$	0.060
R_{int}	0.076
$\Delta\rho_{\text{max}}, \Delta\rho_{\text{min}}$ ($\text{e}/\text{\AA}^3$)	0.18, –0.12



Scheme 1 Synthetic pathway for the synthesis of the target compound.

0.93, 0.97 and 0.96 Å for CH, CH₂ and CH₃ atoms, respectively. The general purpose crystallographic tool PLATON [32] was used for the structure analysis and presentation of the results. The program ORTEP-3 [33] for Windows was used in the preparation of the figures. Details of the data collection conditions and the parameters of the refinement process are given in Table 1.

2.4. Details of the theoretical calculation

All calculations were performed using Gaussian 03 package [34] and Gauss-View molecular visualization software [35] on the personal computer without restricting any symmetry for the title. For modeling, the initial guess of the compound was first obtained from the X-ray coordinates and this structure was optimized by the Density Functional Theory (DFT)/B3LYP method with 6-31G(d, p) and 6-31G+(d, p) as basis sets. From the optimized geometry of the molecule, geometric parameters (bond lengths, bond angles, torsion angles) for the title compound have been calculated theoretically and compared with those of experimental data. The theoretical harmonic frequencies have been calculated in ground state on the optimized molecule. Theoretical harmonic vibrational frequencies were applied to the scale factor which are

0.9608 and 0.9648 for B3LYP/6-31G(d, p) and B3LYP/6-31+G(d, p). These calculated frequencies were compared with the experimental frequencies. The theoretical GIAO ¹H and ¹³C chemical shift values (with respect to TMS) were calculated using the same methods and compared with experimental ¹H and ¹³C chemical shifts. The ¹H- and ¹³C-NMR chemical shifts are converted to the TMS scale by subtracting the calculated absolute chemical shielding of TMS ($\delta = \Sigma_0 - \Sigma$), where δ is the chemical shift, Σ is the absolute shielding and Σ_0 is the absolute shielding of TMS, whose values are 31.75 and 192.06 ppm for B3LYP/6-31G(d, p), 31.64 and 193.08 ppm for B3LYP/6-31+G(d, p), respectively. Besides, molecular electrostatic potential (MEP), frontier molecular orbitals (FMOs), Mulliken population analysis, thermodynamic properties and non-linear optical (NLO) properties of the title molecule were investigated by theoretical calculations.

3. Results and discussion

3.1. Structural description of the compound

The molecular structure of N-(4-(3-methyl-3-phenylcyclobutyl)-3-phenylthiazole-2(3H)-ylidene)aniline with the atom numbering scheme is shown in Fig. 1. The compound is

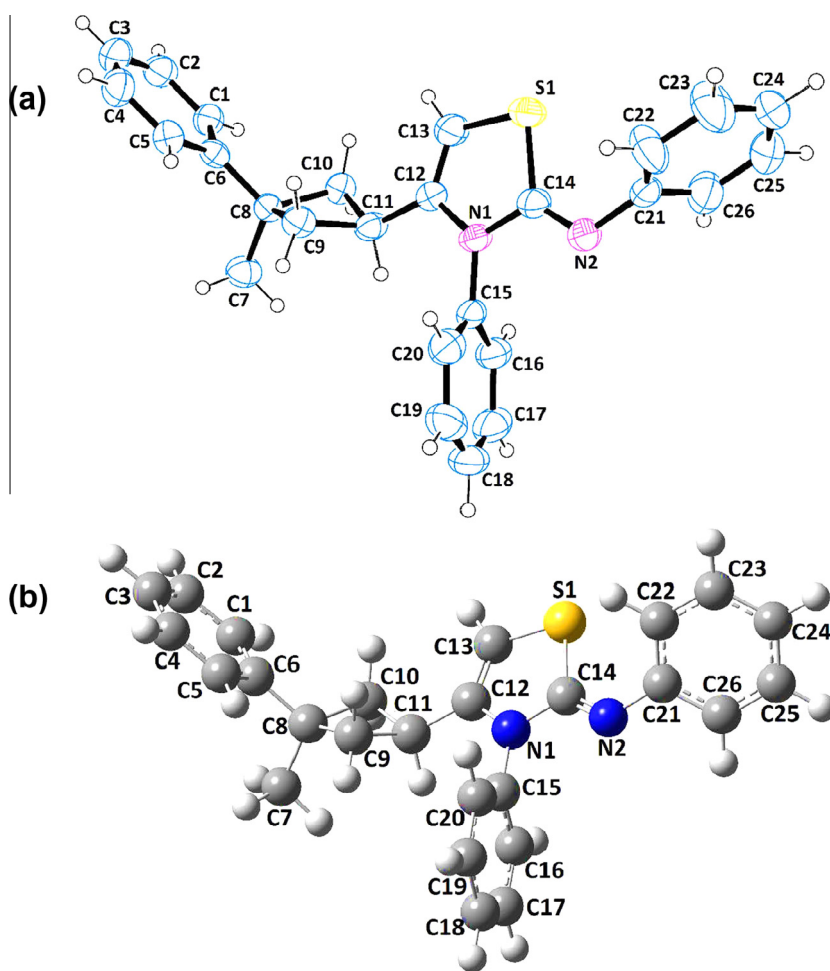


Figure 1 (a) A view of the title compound showing the atom-numbering scheme. Displacement ellipsoids are drawn at the 30% probability level (b) The theoretical geometric structure of the title compound (B3LYP/6-31G+(d, p) level).

monoclinic having the space group $Pca2_1$, with four molecules per unit cell ($Z = 4$) with following dimensions $a = 34.7637$ (19) Å, $b = 5.9235$ (2) Å, $c = 10.4336$ (4) Å.

The structure of molecule contains a cyclobutane, a thiazole and three phenyl rings. Cyclobutane ring is adopted as butterfly conformation. Bond lengths between the carbon atoms are average 1.543 Å and bond angles formed by the three carbons are average 88.4° for the cyclobutane ring in the compound. When these values are compared with the previously reported cyclobutane derivatives [36–43], it is seen that there are no significant differences.

In the thiazole ring, the S1–C13 and S1–C14 bond lengths are 1.735 (3) Å and 1.763 (3) Å. These values are shorter than the accepted values for an S–C sp^2 single bond (1.76 Å) [44]. The C12=C13 bond length [1.393 (3) Å] compares with a literature value of 1.347 (3) Å [43]. The thiazole ring is planar with a maximum deviation of 0.0144 Å.

In crystal structure, the molecules are linked to one another in a zigzag arrangement via C25–H25···N2 hydrogen bonding (Fig 2). The crystal structure is also stabilized by C–H··· π interactions between the C13 atom and C1–C6 rings [symmetry code: (b) $-x, -y, z + 1/2$] and between the C22 atom and

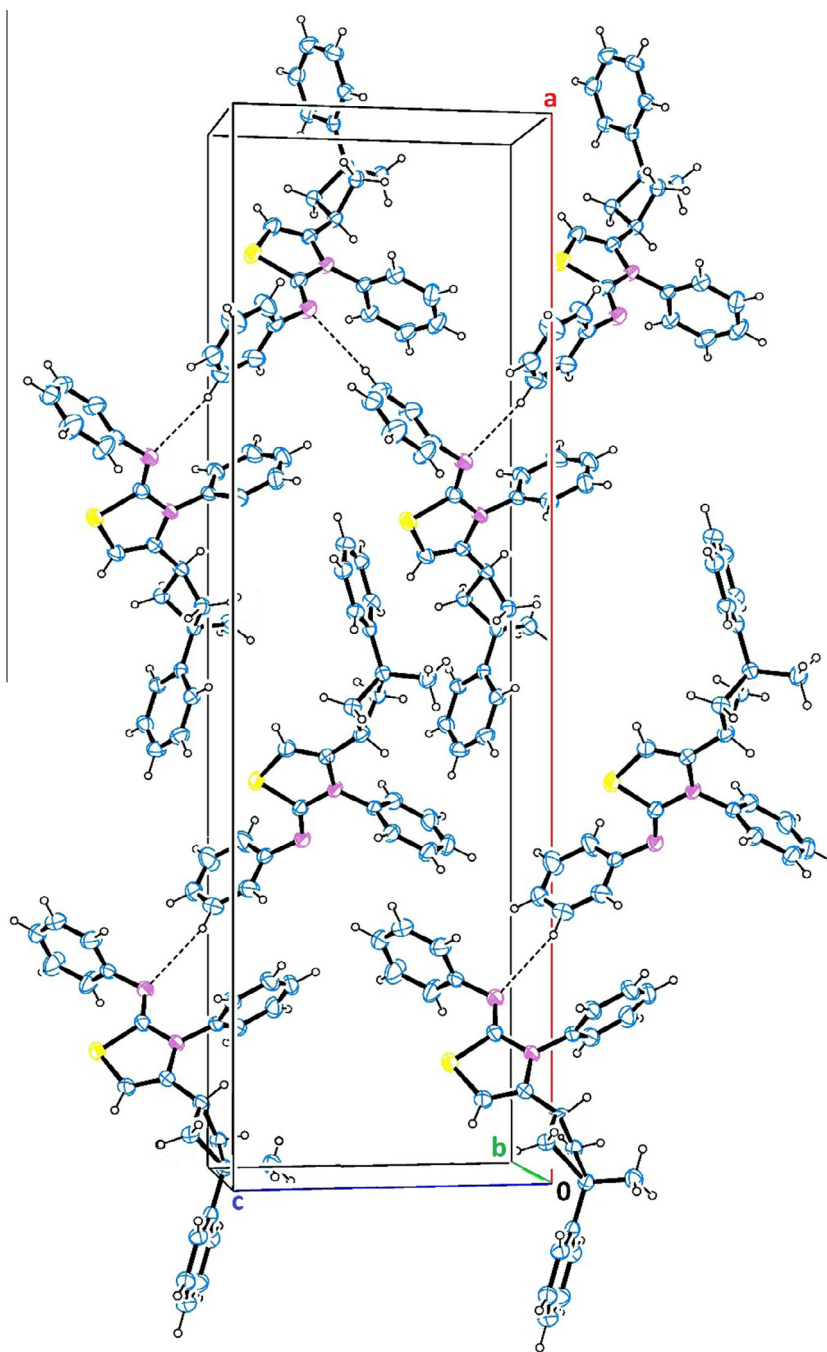


Figure 2 Crystal packing, showing zigzag arrangement of molecules along the c axis. The intermolecular C25–H25···N2 hydrogen bonding is represented by a dashed line.

S1, N1, C12–C14 rings [symmetry code: (c) $x, y + 1, z$]. Details of these hydrogen bonds are given in Table 2. There are no remarkable intramolecular interactions in the crystal structure of the title compound.

3.2. Spectroscopic characterization

3.2.1. Vibrational spectra

The title compound belongs to C1 point group symmetry and consists of 53 atoms. It has seen 153 normal modes of vibrations using the formula $3N-6$. The fundamental vibrational wavenumbers of compound are calculated by DFT/B3LYP/6-31G(d, p) and DFT/B3LYP/6-31G+(d, p) methods. The vibrational band assignments have been made using Gauss View molecular visualization program [35]. The superimposed experimental and scaled theoretical FT-IR spectra of the title compound are given in Fig. 3. In the infrared spectra of the title compound, some observed and calculated frequencies are given in Table 3. Also, some experimentally obtained vibrational frequencies were supported by literature values.

3.2.1.1. Thiazole ring vibrations. The organic compounds containing thiazole ring has specific four bands in FT-IR spectra.

Table 2 Hydrogen-bond geometry (Å, °).

D—H...A	D—H	H...A	D...A	D—H...A
C25—H25...N2 ^a	0.93	2.75	3.597 (4)	151
C13—H13...Cg1 ^b	0.93	2.91	3.603 (3)	133
C22—H22...Cg2 ^c	0.93	2.85	3.725 (3)	156

Symmetry codes: (a) $-x + 1/2, y, z + 1/2$; (b) $-x, -y, z + 1/2$; (c) $x, y + 1, z$.

Cg1 is the centroid of the C1–C6 ring.

Cg2 is the centroid of the S1, N1, C12–C14 ring.

Table 3 Comparison of the observed and calculated vibrational spectra of the title compound.

Assignment	Experimental IR with KBr (cm ⁻¹)	Calculated (cm ⁻¹)	
		B3LYP/6-31G(d, p)	B3LYP/6-31G+(d, p)
vC—H _{thiazole}	3116	3158	3169
v _s C—H _{aromatic}	—	3080	3092
v _{as} C—H _{aromatic}	3049	3072	3088
v _{as} C—H _{2cyclobutane}	3021	3010	3016
v _{as} C—H _{2cyclobutane}	3021	3005	3012
vC—H _{cyclobutane}	2913	2948	2962
v _s C—H _{2cyclobutane}	2961	2953	2959
v _s C—H _{2cyclobutane}	2961	2947	2954
v _s C—H _{3cyclobutane}	2858	2918	2924
vC=N	1621	1641	1633
vC=C _{thiazole}	1578	1598	1594
vC=C _{aromatic}	—	1582	1560
αC—H _{2cyclobutane}	1444	1457	1455
αC—H _{2cyclobutane}	1444	1429	1429
v _s C—H _{3cyclobutane}	1389	1367	1365
γC—H _{cyclobutane}	1323	1356	1358
vC—N	1303	1299	1300
vC—N	1272	1264	1264
γC—H _{cyclobutane}	1223	1223	1221
ωC—H _{2cyclobutane}	1178	1196	1199
δC—H _{2cyclobutane}	1025	1025	1025
ΓC—H _{aromatic}	954	961	956
ΓC—H _{aromatic}	954	958	950
ΓC—H _{aromatic}	954	948	947
ΓC—H _{aromatic}	954	935	940
θ _{cyclobutane}	910	930	932
vS—CH	766	821	824
ΓC—H _{thiazole}	700	687	684

Vibrational modes: v, stretching; α, scissoring; γ, rocking; ω, wagging; δ, twisting; θ, ring breathing; Γ, out-of-plane bending. Abbreviations: s, symmetric; as, asymmetric.

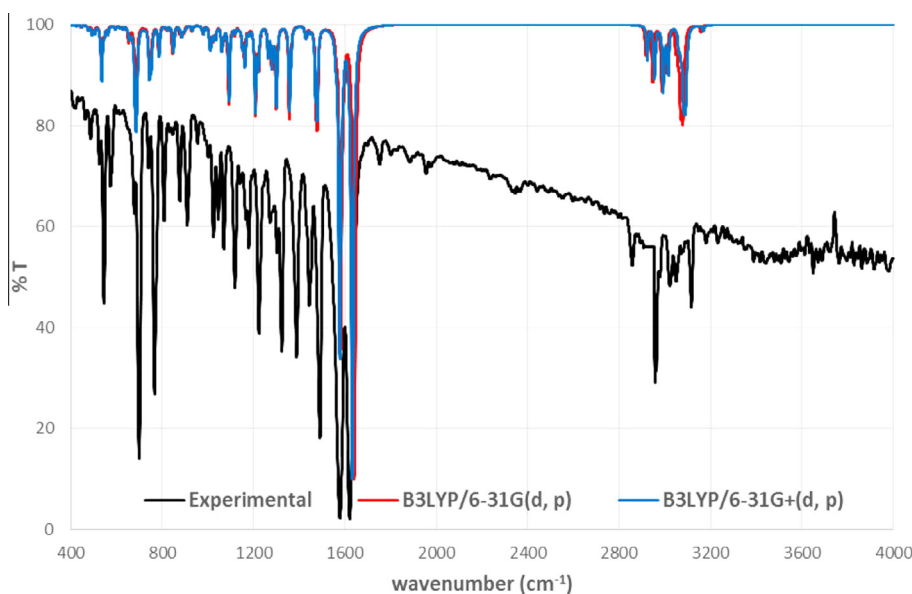


Figure 3 Simulated and experimental FT-IR spectra of the title compound.

These bands are C—H stretching, C=C stretching, S—CH stretching and C—H out-of-plane bending vibrations. The C—H stretching vibration was observed at 3116 cm^{-1} in FT-IR spectrum. In a previous study, the C—H stretching vibration observed 3104 cm^{-1} [39]. The C=C stretching absorption peak observed at 1578 cm^{-1} in FT-IR spectrum and its corresponding calculated frequencies are 1598 and 1594 cm^{-1} using B3LYP/6-31G(d, p) and B3LYP/6-31G+(d, p) levels, respectively. The S—CH stretching and C—H

out-of-plane bending vibrations are recorded at 766 and 700 cm^{-1} , respectively.

3.2.1.2. Cyclobutane ring vibrations. In the title molecule, there are many vibrations of cyclobutane ring. The asymmetric stretching C—H₂ was observed at 3021 cm^{-1} in the FT-IR spectrum and theoretically calculated at 3010 , 3005 and 3016 , 3012 cm^{-1} , respectively. In our previous study [38], this vibration occurred at 2957 cm^{-1} and calculated at 3036 and

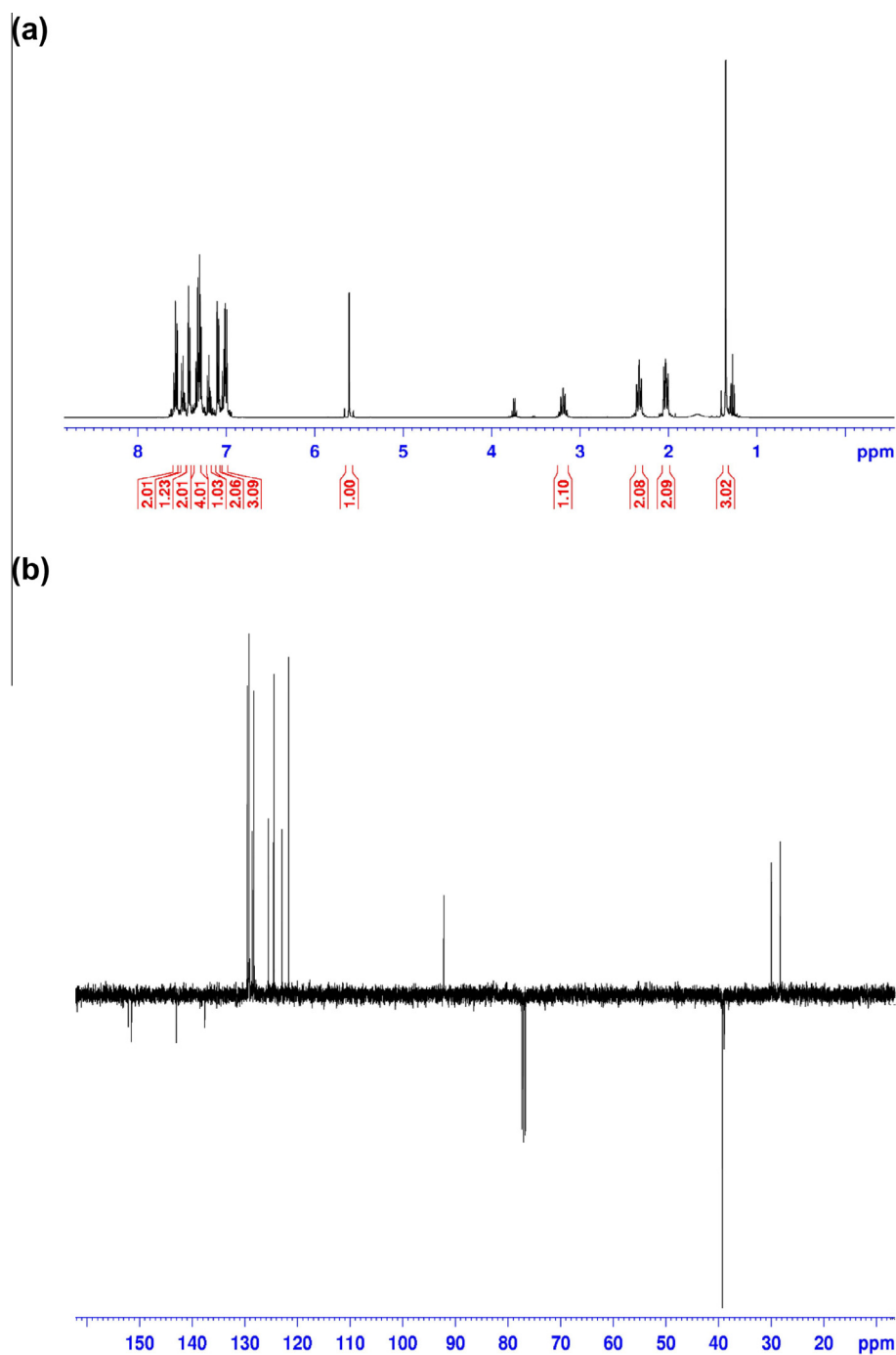


Figure 4 Experimental (a) ^1H and (b) ^{13}C NMR spectra of the title compound.

3015 cm^{-1} for HF/6-31G(d) and B3LYP/6-31G(d) levels, respectively. Similarly, the symmetric stretching C—H₂ observed at 2961 cm^{-1} in FT-IR spectrum and theoretically calculated at 2953, 2947 and 2959, 2954 cm^{-1} , respectively. The scissoring C—H₂, wagging C—H₂, and twisting C—H₂ vibrations are observed respectively at 1444, 1178 and 1025 cm^{-1} in the FT-IR spectrum for the cyclobutane ring.

Another characteristic vibration of the cyclobutane ring is breathing, which is shrinkage and enlargement of the ring. The breathing assignment of cyclobutane can be observed at the range of 900–1100 cm^{-1} in the FT-IR spectrum. In the infrared spectra of the title compound, a band is observed at 910 cm^{-1} for this vibration.

3.2.1.3. Phenyl ring vibrations. The aromatic organic compound structure; benzene and its derivatives show the presence of asymmetric C—H stretching vibrations in the region 3100–3000 cm^{-1} [45–47] which is the characteristic region for the recognition of C—H stretching vibrations. In the title molecule, these vibrations have been observed at the region 3057–3025 cm^{-1} in experimental spectrum and calculated at regions 3092–3048 cm^{-1} and 3085–2979 cm^{-1} for B3LYP/6-31G(d, p) and 6-31G+(d, p) levels, respectively. The experimental and theoretical regions were found to be consistent with the literature values. The out of plane C—H bending was observed at 954 cm^{-1} in the FT-IR spectrum and theoretically calculated at regions 961–935 (B3LYP/6-31G(d, p)) and 956–940 (B3LYP/6-31G+(d, p)) cm^{-1} , which are found to be well within their characteristic region. These frequencies are compatible with two literature values of 941 and 839 cm^{-1} [48].

3.2.2. NMR spectra

The compound was also characterized by the use of ¹H and ¹³C NMR spectroscopies. The ¹H and ¹³C NMR spectra of the title compound were recorded using TMS as an internal standard and chloroform (CDCl₃) as solvent and are shown in Fig. 4a and b. GIAO ¹H and ¹³C chemical shift values (with respect to TMS) were calculated using the DFT (B3LYP) method with the 6-31G(d, p) and 6-31+G(d, p) basis sets and compared with experimental ¹H and ¹³C chemical shift values. The results of this calculation are shown in Table 4 together with experimental values.

It is well known that the hydrogen atoms of aromatic organic compounds and derivatives show the presence of chemical shifts in the region 6.5–7.5 ppm. For the title compound, experimentally these chemical shifts have been seen at region 7.02–7.57 ppm and calculated at region 6.43–7.84 and 6.91–8.08 ppm for B3LYP/6-31G(d, p) and 6-31G+(d, p) levels, respectively. The proton chemical shifts of the —CH₂— group in the cyclobutane ring have been recorded at an average of 2.28 ppm. Also, >CH— signals of the cyclobutane have been observed at 3.19 ppm with a J-coupling value of 9.2 Hz. Thiazole ring has one hydrogen atom and proton NMR chemical shift and J-coupling value for this hydrogen atom have been presented 5.61 ppm and 1.6 Hz, respectively.

In the ¹³C NMR spectra, for the cyclobutane ring, a single peak was observed belonging to C9 and C10 at 39.27 ppm, because they have the same chemical environment. These signals have been calculated at 42.08 and 36.95 ppm for the

Table 4 Experimental and theoretical (¹³C and ¹H) isotropic chemical shifts (ppm) for the title compound.

Atom	Experimental	B3LYP/ 6-31G(d, p)	B3LYP/ 6-31G+(d, p)
C1	124.53	119.71	125.68
C2	128.64	123.05	135.05
C3	125.57	120.44	123.44
C4	128.64	123.07	124.23
C5	124.53	119.79	123.99
C6	137.68	148.23	151.63
C7	28.29	31.25	32.73
C8	38.91	43.52	48.21
C9	39.27	42.08	42.16
C10	39.27	36.95	37.77
C11	29.98	30.88	32.77
C12	151.54	137.38	142.32
C13	92.22	93.82	96.36
C14	152.1	155.14	157.66
C15	129.55	135.17	138.23
C16	123.56	123.98	127.48
C17	129.2	124.52	125.88
C18	122.96	123.7	126.12
C19	129.2	124.49	126.07
C20	123.56	126.81	131.39
C21	143.07	145.93	149.56
C22	121.71	111.79	114.01
C23	129.25	123.79	125.98
C24	128.32	116.99	118.70
C25	129.25	123.93	125.51
C26	121.71	118.88	120.81
H1	7.57	7.53	7.29
H2	7.48	7.51	7.77
H3	7.42	7.43	7.36
H4	7.48	7.46	7.66
H5	7.57	7.14	7.33
H7A	1.35	0.89	0.95
H7B	1.35	1.47	1.48
H7C	1.35	1.08	0.95
H9A	2.09	1.99	2.1
H9B	2.36	1.65	1.83
H10A	2.34	2.54	2.59
H10B	2.34	2.39	2.46
H11 (<i>j</i> = 9.2 Hz)	3.19	3.25	3.32
H13 (<i>j</i> = 1.6 Hz)	5.61	5.54	6.01
H16	7.02	7.48	7.61
H17	7.31	7.84	8.08
H18	7.09	7.74	7.84
H19	7.31	7.76	8.06
H20	7.02	7.67	7.52
H22	7.09	7.36	7.48
H23	7.57	7.44	7.63
H24	7.20	7.11	7.22
H25	7.57	7.39	7.47
H26	7.09	6.43	6.91

6-31G(d, p) level and at 42.16 and 37.77 ppm for 6-31G+(d, p) level, respectively.

¹³C NMR spectra of the thiazole compound show the signals at 92.22 (C13) and 152.1 (C14) ppm due to C atoms next to sulfur atom. These signals have been found as 111.52 and 167.57 ppm in the literature [39] as well as have

been calculated as 93.82 and 155.14 ppm for B3LYP/6-31G(d, p) level and 96.36 and 157.66 ppm for B3LYP/6-31G+(d, p) level.

Table 5 Theoretically computed some parameters for the molecule.

Parameters	B3LYP/ 6-31G(d, p)	B3LYP/ 6-31G+(d, p)
Total energy (a.u.)	-1512.91705601	-1512.95360279
Zero-point vibrational energy (kcal/mol)	271.95395	271.36885
Entropy (cal/mol-K)	178.2	178.180
Heat capacity at const. volume (CV, cal/mol-K)	98.498	98.713
<i>Rotational constants (GHz)</i>		
A	0.27115	0.27196
B	0.07800	0.07744
C	0.06745	0.06687
<i>Dipole moment (Debye)</i>		
μ_x	3.6251	3.6482
μ_y	1.7256	1.6703
μ_z	-0.3666	-0.4271
μ_{top}	4.0316	4.0351

Table 6 Some selected geometric parameters (Å, °).

Geometric Parameters	Experimental [X-ray diffraction]	Calculated	
		B3LYP/ 6-31G(d, p)	B3LYP/ 6-31G+(d, p)
<i>Bond lengths (Å)</i>			
C1—C2	1.391 (3)	1.395	1.397
C2—C3	1.375 (4)	1.394	1.397
C6—C8	1.515 (3)	1.518	1.518
C7—C8	1.532 (3)	1.540	1.541
C8—C9	1.545 (3)	1.563	1.563
C11—C12	1.486 (3)	1.496	1.497
C12—C13	1.325 (3)	1.347	1.349
C12—N1	1.407 (3)	1.409	1.410
C13—S1	1.736 (3)	1.761	1.761
S1—C14	1.763 (3)	1.801	1.803
C14—N2	1.269 (3)	1.276	1.278
N2—C21	1.414 (3)	1.399	1.400
C21—C22	1.364 (3)	1.408	1.409
C22—C23	1.380 (4)	1.391	1.397
N1—C15	1.439 (3)	1.436	1.438
C15—C16	1.368 (3)	1.397	1.397
C16—C17	1.383 (4)	1.396	1.397
<i>Bond angles (°)</i>			
C8—C9—C11	89.05 (18)	88.8	88.82
C8—C10—C11	89.05 (18)	89.19	89.23
C12—N1—C14	115.0 (2)	115.66	115.62
C13—S1—C14	90.46 (14)	90.63	90.66
C14—N2—C21	116.7 (2)	123.59	123.78
C20—C15—C16	120.7 (3)	120.29	120.36
<i>Torsion angles (°)</i>			
C8—C9—C11—C10	19.1 (2)	17.76	17.72
C9—C8—C10—C11	19.01 (19)	17.75	17.7
C20—C15—N1—C14	80.2 (3)	76.88	79.7
N1—C12—C11—C9	94.4 (3)	72.31	72.73
C5—C6—C8—C7	99.2 (3)	89.59	89.31
S1—C14—N1—C15	175.42 (19)	177.67	178.11

3.3. Quantum-chemical studies

3.3.1. Structural optimization

The molecular structure of the title compound was also calculated theoretically. The starting geometry was that obtained from the X-ray structure determination optimized using the Density Functional Theory (DFT/B3LYP) method with the 6-31G(d, p) and 6-31G+(d, p) basis sets in ground state. The total energy, zero-point vibrational energy, entropy and dipole moment values obtained for optimized geometries are presented in Table 5.

The Density Functional Theory (DFT) modeling method gives quite accurate results in calculation of the molecular geometry. Conventionally, two methods were used for comparing the molecular structures. The first method is to calculate the correlation value (R^2). The optimized geometrical parameters (bond lengths, bond angles and torsion angles) calculated by B3LYP/6-31G(d, p) and B3LYP/6-31+G(d, p) methods are listed in Table 6. Calculated R^2 values are 0.9892 and 0.9891 for bond lengths, 0.9769 and 0.9759 for bond angles, 0.9774 and 0.9766 for torsion angles at B3LYP/6-31G(d, p) and B3LYP/6-31+G(d, p) levels, respectively. According to correlation values, the B3LYP/6-31G(d, p) method gave accurate results for the bond lengths, bond angles, torsion angles compared with the B3LYP/6-31G+(d, p) method.

The second method, comparing the structures obtained with the theoretical calculations is by superimposing the molecular skeleton with that obtained from X-ray diffraction, giving a RMSE of 0.596 Å and 0.599 Å for B3LYP/6-31G(d, p) and B3LYP/6-31+G(d, p) levels, respectively (Fig. 5). According to these results, it may be concluded that the

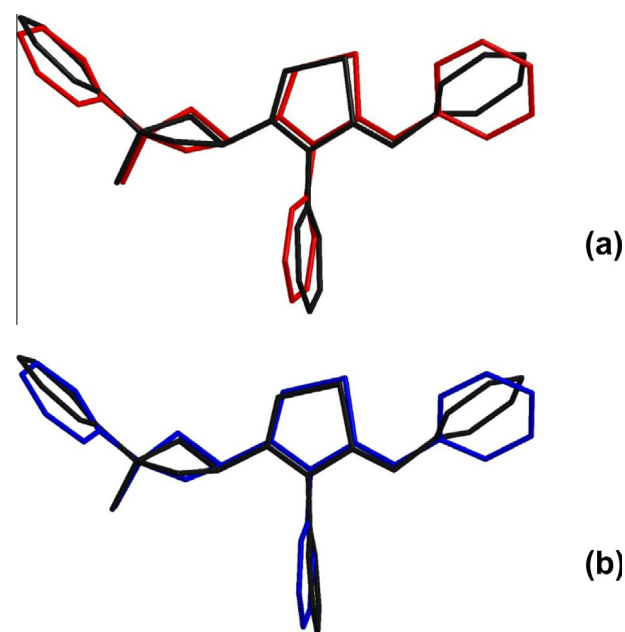


Figure 5 Atom-by-atom superimposition of the structures calculated (red) [a = B3LYP/6-31G(d, p), b = B3LYP/6-31G+(d, p)] over the X-ray structure (black) for the title compound. Hydrogen atoms omitted for clarity.

B3LYP/6-31G(d, p) calculation well reproduced the geometry of the title compound. While making these comparisons, it should not be forgotten that the calculations were carried out in the gas phase.

3.3.2. Molecular electrostatic potential (MEP)

A molecule of electrostatic potential map provides information about the electron acceptor and electron-donor regions. Using this information, we can estimate intramolecular and intermolecular hydrogen bonds may present between the atoms. The different values of the electrostatic potential at the surface are represented by different colors; red represents regions of most electro negative electrostatic potential, blue represents regions of most positive electrostatic potential and green represents regions of zero potential.

The molecular electrostatic potential maps were calculated at the B3LYP/6-31G(d, p) and B3LYP/6-31+G(d, p) levels. The color code of these maps is in the range from -0.052 a.u. (red) to 0.052 a.u. (blue) for B3LYP/6-31G(d, p), -0.049 a.u. (red) to 0.049 a.u. (blue) for B3LYP/6-31G(d, p) in Fig. 6. In here, the red regions settled in N2 atom. So, N2 atom can be estimated to be electron-donors. This estimate was confirmed by the C25—H25...N2 hydrogen-bonding in the crystal structure.

3.3.3. HOMO and LUMO analysis

The distributions of the HOMO and LUMO orbitals computed for the B3LYP/6-31G(d, p) and B3LYP/6-31G+(d, p) levels for the title compound are shown in Fig. 7. The calculations indicate that the title compound has 105 occupied molecular orbitals and the value of the HOMO and LUMO energies are -4.95 and -0.51 eV for B3LYP/6-31G(d, p) level, -5.23 and -0.91 eV for B3LYP/6-31G+(d, p) level, respectively. Using HOMO and LUMO energy values for a molecule, electronegativity, chemical hardness and chemical softness can be calculated as follows:

$$\chi = (I + A)/2 \text{ (electronegativity),}$$

$$\eta = (I - A)/2 \text{ (chemical hardness),}$$

$$S = 1/2\eta \text{ (chemical softness)}$$

where I and A are ionization potential and electron affinity;

$$I = -E_{\text{HOMO}}$$

$$A = -E_{\text{LUMO}}$$

respectively [49]. The HOMO and LUMO energies, the ionization potential (I), the electron affinity (A), the absolute electronegativity (χ), the absolute hardness (η) and softness (S)

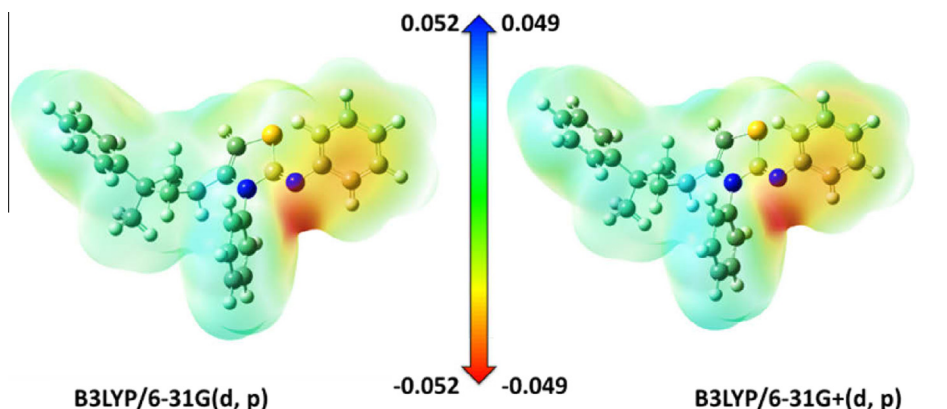


Figure 6 Molecular electrostatic potential map calculated at B3LYP/6-31G(d, p) and B3LYP/6-31G+(d, p) levels.

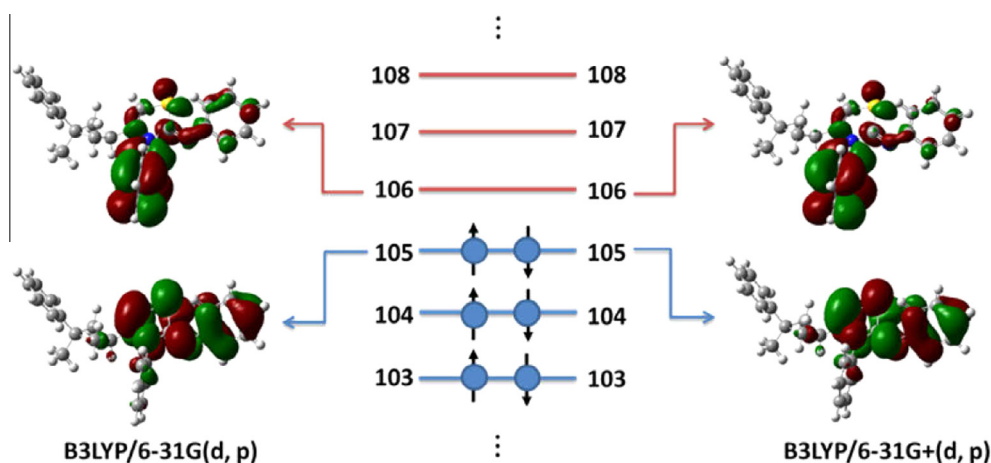


Figure 7 Molecular orbitals and energies for the HOMO and LUMO of the title compound.

for molecule have been calculated at the same levels and the results are given in Table 7.

3.3.4. Mulliken population analysis

The charge distributions were calculated by the Mulliken method [50] for the equilibrium geometry of the title compound. The corresponding Mulliken's plot is shown in Fig. 8. The Mulliken charges of the atoms in hydrogen bondings and the sum of atoms belonging to the rings are shown in Table 8. These charge as theoretically calculated was verified by C—H...N and C—H... π interactions in the crystal structure of compound.

3.3.5. Thermodynamic properties

In order to determine thermodynamical properties of the title compound, the standard thermodynamic functions, entropy

(S_m^0), heat capacity ($C_{p,m}^0$) and enthalpy (H_m^0) based on the vibrational analysis at B3LYP/6-31G(d, p) and B3LYP/6-31G+(d, p) levels and statistical thermodynamics for the title compound were obtained and listed in Table 9.

As can be seen from the table, the entropies, standard heat capacities, and enthalpies increase at any temperature from 100 K to 1000 K since increasing temperature causes an increase in the intensity of the molecular vibration and the populations of the excited vibrational states. According to the data in Table 9 for the title compound, the correlation equations between the thermodynamic properties and temperature T , which can be used for the further studies of the title compound, are as follows (Fig. 9):

For B3LYP/6-31G(d, p) level;

$$S_m^0 = -8E - 05T^2 + 0.4002T + 70.528 \quad (R^2 = 1)$$

$$C_{p,m}^0 = -0.0002T^2 + 0.4226T + 4.9418 \quad (R^2 = 0.999)$$

$$H_m^0 = 0.0001T^2 + 0.0397T - 4.265 \quad (R^2 = 0.9994)$$

For B3LYP/6-31G+(d, p) level;

$$S_m^0 = -8E - 05T^2 + 0.4012T + 69.947 \quad (R^2 = 0.9999)$$

$$C_{p,m}^0 = -0,0002T^2 + 0.422T - 4.9538 \quad (R^2 = 0.999)$$

$$H_m^0 = 0.0001T^2 + 0.0395T - 4.2463 \quad (R^2 = 0.9994)$$

3.3.6. Non-linear optical effects

The linear polarizability (α_{tot}) and first-order hyperpolarizability (β_{tot}) of the title compound were calculated at the

Table 7 The calculated frontier orbital energies, electronegativity, hardness and softness of compound using B3LYP/6-31G(d, p) and B3LYP/6-31G+(d, p) levels.

	B3LYP/6-31G(d, p)	B3LYP/6-31G+(d, p)
E_{HOMO} (eV)	-4.95	-5.22
E_{LUMO} (eV)	-0.51	-0.91
I (eV)	4.95	5.22
A (eV)	0.51	0.91
χ (eV)	2.73	3.07
η (eV)	2.22	2.16
S (eV)	0.23	0.23

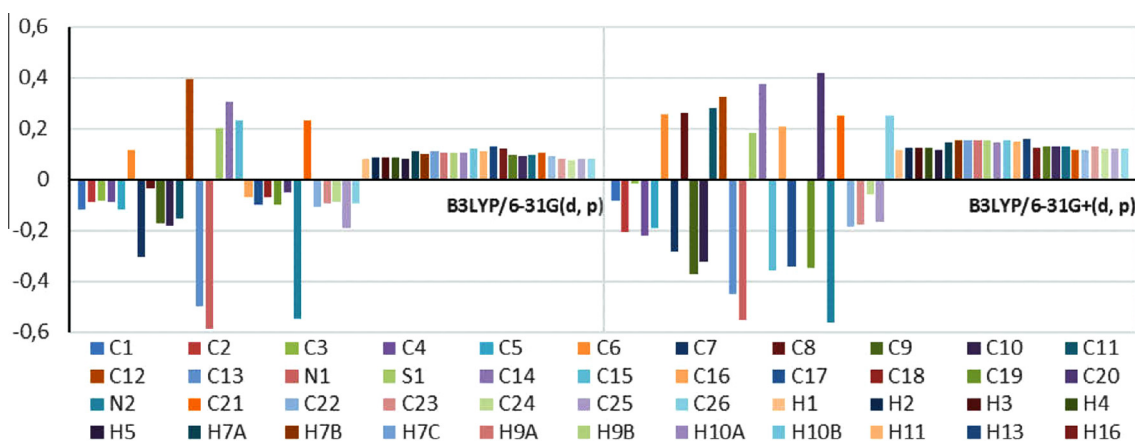


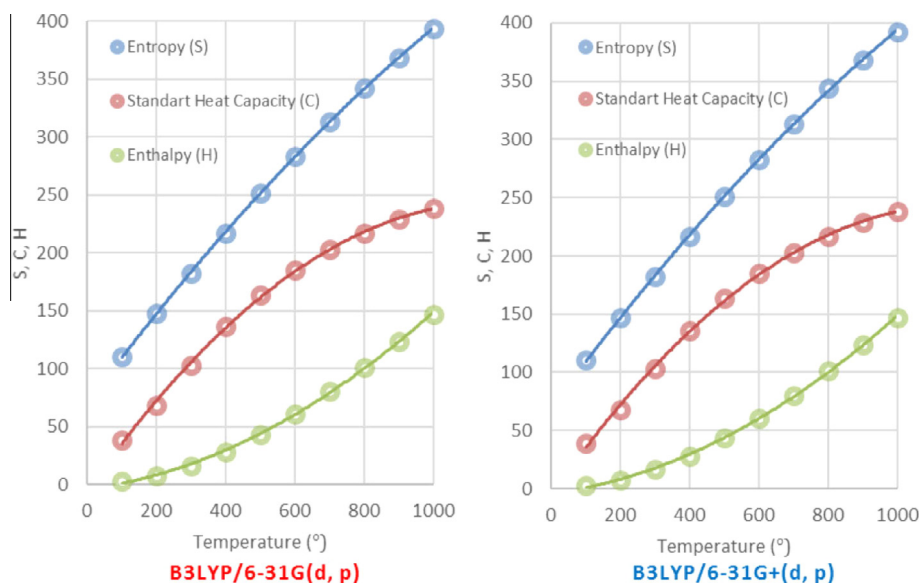
Figure 8 Charge distribution calculated by the Mulliken method for compound.

Table 8 Mulliken charges of the atoms in hydrogen bonding for the title compound.

D—H...A	B3LYP/6-31G(d, p)			B3LYP/6-31G+(d, p)		
	D	H	A	D	H	A
C25—H25...N2	-0.193	0.079	-0.551	-0.168	0.121	-0.564
C—H...Cg	D	H	Cg	D	H	Cg
C13—H13...Cg1	-0.499	0.128	-0.388	-0.451	0.157	-0.463
C22—H22...Cg2	-0.111	0.092	-0.187	-0.188	0.116	-0.125

Table 9 Thermodynamic properties of the title compound at different temperatures.

T (°C)	Entropy (S)		Standard Heat Capacity (C)		Enthalpy (H)	
	B3LYP/6-31G(d, p)	B3LYP/6-31G+(d, p)	B3LYP/6-31G(d, p)	B3LYP/6-31G+(d, p)	B3LYP/6-31G(d, p)	B3LYP/6-31G+(d, p)
100	110,567	110,269	38,798	38,786	2,479	2,474
200	147,547	147,203	68,484	68,351	7,784	7,772
300	182,632	182,216	103,247	103,038	16,356	16,326
400	217,532	217,056	136,217	136,011	28,368	28,317
500	251,424	250,904	163,611	163,418	43,409	43,338
600	283,621	283,068	185,429	185,265	60,902	60,814
700	313,871	313,294	202,895	202,739	80,349	80,246
800	342,187	344,021	217,107	216,953	101,373	101,254
900	368,692	368,078	228,862	228,708	123,689	123,555
1000	393,539	392,909	238,704	238,551	147,081	146,932

**Figure 9** Thermodynamic properties of the title compound at different temperatures.**Table 10** Calculated polarizability and the first hyperpolarizability components (a.u.) for the title compound.

	B3LYP/6-31G(d, p)	B3LYP/6-31G+(d, p)
α_{xx}	256.07	297.28
α_{xy}	-36.63	-38.93
α_{yy}	315.48	359.3
α_{xz}	-37.77	-40.62
α_{yz}	22.54	28.96
α_{zz}	335.45	377.49
$\alpha_{tot.}$	302.33	344.68
β_{xxx}	43.94	-38.27
β_{xxy}	123.19	191.23
β_{xyy}	-231.44	-190.53
β_{yyy}	57.91	159.21
β_{xxz}	-39.74	17.38
β_{xyz}	-157.28	-150.48
β_{yyz}	272.51	253.33
β_{xzz}	54.82	-10.12
β_{yzz}	67.45	72.19
β_{zzz}	-137.7	-178.2
$\beta_{tot.}$	297.35	494.22

B3LYP/6-31G(d, p) and B3LYP/6-31G+(d, p) levels. The values of the polarizability α and the first hyperpolarizability β of Gaussian 03 output are reported in atomic units (a.u.). The components of the polarizability and first hyperpolarizability are given in Table 10. The calculated values of α_{tot} and β_{tot} are 302.33, 297.35 and 344.68, 494.22 a.u., respectively. Urea is one of the prototypical molecules used in the study of the NLO properties of molecular systems. Therefore it was used frequently as a threshold value for comparative purposes. The values of α_{tot} and β_{tot} of urea are 25.99, 73.6 and 33.1, 59.4 a.u. obtained at the same levels. Theoretically, the first-order hyperpolarizability of the title compound is of 4.68 and 8.32 times the magnitude of urea. According to these results, the title compound is a good candidate of NLO material.

4. Conclusions

In this study, N-(4-(3-methyl-3-phenylcyclobutyl)-3-phenylthiazole-2(3H)-ylidene)aniline, ($C_{26}H_{24}N_2S$), was prepared and investigated by spectroscopic (FT-IR and NMR) and

structural (single-crystal X-ray diffraction) methods. To support the experimental findings, the geometric parameters, vibrational assignments and ^1H and ^{13}C NMR chemical shifts of the title compound have been calculated using the density functional theory DFT (B3LYP) method with the 6-31+G(d, p) basis set, and compared with the experimental data. When the geometric parameters, vibrational frequencies and chemical shifts of the compound are compared with experimental data, it is seen that there are no significant differences. It was noted here that the experimental results belong to solid phase and theoretical calculations belong to gaseous phase. In the solid state, the existence of the crystal field along with the intermolecular interactions have connected the molecules together, which result in the differences of bond parameters between the calculated and experimental values. The calculated molecular electrostatic potential map confirmed the solid-state interactions. The predicted non-linear optical (NLO) properties of the title compound are much greater than those of urea. The title compound is a good candidate as second-order non-linear optical material.

Acknowledgments

We are grateful to Firat University Scientific Research Coordination Center (FUBAP Project No: FF.12.12) for financial support of this work. I wish to thank Prof. Dr. Orhan Büyükgüngör for his help with the data collection and acknowledge the Faculty of Arts and Sciences, Ondokuz Mayıs University, Turkey, for the use of the STOE IPDS II diffractometer.

References

- [1] A. Kumar, C.S. Rajput, S.K. Bhati, *Bioorg. Med. Chem.* 15 (2007) 3089–3096.
- [2] B.S. Holla, K.V. Malini, B.S. Rao, B.K. Sarojini, N.S. Kumari, *Eur. J. Med. Chem.* 38 (2003) 313–318.
- [3] F. Azam, I.A. Alkskas, S.L. Khokra, O. Prakash, *Eur. J. Med. Chem.* 44 (2009) 203–211.
- [4] K.M. Dawood, H.A. Gawad, E.A. Rageb, M. Ellithey, H.A. Mohamed, *Bioorg. Med. Chem.* 14 (2006) 3672–3680.
- [5] F. Chimenti, B. Bizzarri, E. Maccioni, D. Secci, A. Bolasco, R. Fioravanti, P. Chimenti, A. Granese, S. Carradori, D. Rivanera, D. Lilli, A. Zicari, S. Distinto, *Bioorg. Med. Chem. Lett.* 17 (2007) 4635–4640.
- [6] B. Narayana, K.K. Vijaya Raj, B.V. Ashalatha, N.S. Kumari, B.K. Sarojini, *Eur. J. Med. Chem.* 39 (2004) 867–872.
- [7] G.S. Hassan, S.M. El-Messery, F.A.M. Al-Omary, H.I. El-Subbagh, *Bioorg. Med. Chem. Lett.* 22 (2012) 6318–6323.
- [8] I. Hutchinson, M.S. Chua, H.L. Browne, V. Trapani, T.D. Bradshaw, A.D. Westwell, M.F.G. Stevens, *J. Med. Chem.* 44 (2001) 1446–1455.
- [9] G. Aridoss, S. Amirthagesan, M.S. Kima, J.T. Kim, Y.T. Jeong, *Eur. J. Med. Chem.* 44 (2009) 4199–4210.
- [10] M.R. Shiradkar, K.K. Murahari, H.R. Gangadasu, T. Suresh, C.A. Kalyan, D. Panchal, H. Kaur, P. Burange, J. Ghogare, V. Mokalec, M. Raut, *Bioorg. Med. Chem.* 15 (2007) 3997–4008.
- [11] P. Karegoudar, M.S. Karthikeyan, D.J. Prasad, M. Mahalinga, B.S. Holla, N.S. Kumari, *Eur. J. Med. Chem.* 43 (2008) 261–267.
- [12] O. Bozdog-Dundar, O. Ozgen, A. Mentese, N. Altanlar, O. Ath. E. Kendj, R. Ertan, *Bioorg. Med. Chem.* 15 (2007) 6012–6017.
- [13] P. Vicini, A. Geronikaki, K. Anastasia, M. Incerti, F. Zani, *Bioorg. Med. Chem.* 14 (2006) 3859–3864.
- [14] F. Bordi, P.L. Catellani, G. Morinha, P.V. Plazzi, C. Silva, E. Barocelli, M. Chiavarini, *II Farmaco* 44 (1989) 795.
- [15] A.M. Vijesh, A.M. Isloor, V. Prabhu, S. Ahmad, S. Malladi, *Eur. J. Med. Chem.* 45 (2010) 5460.
- [16] K.D. Hargrave, F.K. Hess, J.T. Oliver, *J. Med. Chem.* 26 (1983) 1158.
- [17] B.A. Steinbaugh, B.L. Batley, C.A. Painchaud, S.T. Rapundalo, B.M. Michniewicz, S.C.J. Olson, *J. Med. Chem.* 35 (1992) 2562.
- [18] S.A.F. Rostom, M.I. El-Ashmawhy, H.A.A. El-Razik, M.H. Badr, H.M.A. Ashour, *Bioorg. Med. Chem.* 17 (2009) 882.
- [19] K. Tsuji, H. Ishikawa, *Bioorg. Med. Chem. Lett.* 4 (1994) 1601.
- [20] F.W. Bell, A.S. Cantrell, M. Hogberg, S.R. Jaskunas, N.G. Johansson, C.L. Jordon, M.D. Kinnick, P. Lind, J.M. Morin, R. Norren, B. Oberg, J.A. Palkowitz, C.A. Parrush, P. Pranc, C. Sahlberg, R.J. Ternansky, P.T. Vasileff, L. Vrang, S.L. West, H. Zhang, X.X. Zhou, *J. Med. Chem.* 38 (1995) 4929.
- [21] T.P.A. Devasagayam, S. De, S. Adhikari, J.K. Jain, V.P. Menon, *Chem. Biol. Interact.* 173 (2008) 215.
- [22] M. Shiradkar, G.V. Suresh Kumar, V. Dasari, S. Tatikonda, K.C. Akula, R. Shah, *Eur. J. Med. Chem.* 42 (2007) 807.
- [23] J.J. Harnett, V. Roubert, C. Dolo, C. Charnet, B. Spinnewyn, S. Cornet, A. Rolland, J.G. Marin, D. Bigg, P.E. Chabrier, *Bioorg. Med. Chem. Lett.* 14 (2004) 157.
- [24] M.H. Shih, F. Ying, Ke, *Bioorg. Med. Chem.* 12 (2004) 4633.
- [25] L.-R. Edward, G. Mladenova, *Chem. Rev.* 103 (2003) 1449–1483 (and references cited therein).
- [26] J.C. Namyslo, D.E. Kaufmann, *Chem. Rev.* 103 (2003) 1485–1537 (and references cited therein).
- [27] < <http://en.wikipedia.org/wiki/Cyclobutane>. >
- [28] E.V. Dehmlow, S. Schmidt, *Liebigs Ann. Chem.* (1990) 411–414.
- [29] Stoe & Cie, X-Area Version 1.18, Stoe & Cie, Darmstadt, 2002.
- [30] G.M. Sheldrick, SHELXS-97; Program for the Solution of Crystal Structures, University of Gottingen, 1997.
- [31] G.M. Sheldrick, SHELXL-97; Program for Crystal Structures Refinement, University of Gottingen, 1997.
- [32] A.L. Spek, *Acta Crystallogr. D* 65 (2009) 148–155.
- [33] L.J. Farrugia, *J. Appl. Cryst.* 45 (2012) 849–854.
- [34] M.J. Frisch, G.W. Trucks, H.B. Schlegel, G.E. Scuseria, M.A. Robb, J.R. Cheeseman, J.A. Montgomery Jr., T. Vreven, K.N. Kudin, J.C. Burant, J.M. Millam, S.S. Iyengar, J. Tomasi, V. Barone, B. Mennucci, M. Cossi, G. Scalmani, N. Rega, G.A. Petersson, H. Nakatsuji, M. Hada, M. Ehara, K. Toyota, R. Fukuda, J. Hasegawa, M. Ishida, T. Nakajima, Y. Honda, O. Kitao, H. Nakai, M. Klene, X. Li, J.E. Knox, H.P. Hratchian, J.B. Cross, V. Bakken, C. Adamo, J. Jaramillo, R. Gomperts, R.E. Stratmann, O. Yazyev, A.J. Austin, R. Cammi, C. Pomelli, J.W. Ochterski, P.Y. Ayala, K. Morokuma, G.A. Voth, P. Salvador, J.J. Dannenberg, V.G. Zakrzewski, S. Dapprich, A.D. Daniels, M.C. Strain, O. Farkas, D.K. Malick, A.D. Rabuck, K. Raghavachari, J.B. Foresman, J.V. Ortiz, Q. Cui, A.G. Baboul, S. Clifford, J. Cioslowski, B.B. Stefanov, G. Liu, A. Liashenko, P. Piskorz, I. Komaromi, R.L. Martin, D.J. Fox, T. Keith, M.A. Al-Laham, C.Y. Peng, A. Nanayakkara, M. Challacombe, P.M.W. Gill, B. Johnson, W. Chen, M.W. Wong, C. Gonzalez, J.A. Pople, Gaussian 03, Revision E.01, Gaussian, Inc., Wallingford, CT, 2004.
- [35] R. Dennington II, T. Keith, J. Millam, Gauss View, Version 4.1.2, Semichem Inc., Shawnee Mission, KS, 2007.
- [36] F. Sen, M. Dinçer, A. Cukurovali, I. Yilmaz, *Acta Cryst. E67* (2011) o958–o959.

- [37] F. Sen, M. Dinçer, A. Cukurovali, I. Yilmaz, *Acta Cryst.* E68 (2012) o1052.
- [38] F. Sen, M. Dinçer, A. Cukurovali, I. Yilmaz, *J. Mol. Struct.* 1046 (2013) 1–8.
- [39] E. Inkaya, M. Dinçer, Ö. Ekici, A. Cukurovali, *J. Mol. Struct.* 1026 (2012) 117–126.
- [40] E. Inkaya, M. Dinçer, Ö. Ekici, A. Cukurovali, *Spectrochim. Acta A* 101 (2013) 218–227.
- [41] N. Özdemir, M. Dinçer, A. Cukurovali, O. Büyükgüngör, *J. Mol. Model.* 15 (2009) 1435–1445.
- [42] N. Özdemir, M. Dinçer, A. Cukurovali, *J. Mol. Model.* 16 (2010) 291–302.
- [43] F. Sen, O. Ekici, M. Dincer, A. Cukurovali, I. Yilmaz, *J. Mol. Struct.* 1086 (2015) 109–117.
- [44] F.H. Allen, *Acta Cryst.* B40 (1984) 64–72.
- [45] G. Socrates, *Infrared Characteristic Group Frequencies*, Wiley Intersciences Publication, New York, 1980.
- [46] F.R. Dollish, W.G. Fateley, F.F. Bentley, *Characteristic Raman Frequencies of Organic Compounds*, John Wiley & Sons, New York, 1997.
- [47] G. Varsanyi, *Vibrational Spectra of Benzene Derivatives*, Academic Press, New York, 1969.
- [48] M. Kandasamy, G. Velraj, *Solid State Sci.* 14 (2012) 1071–1079.
- [49] R.G. Pearson, *Proc. Natl. Acad. Sci. U.S.A* 83 (1986) 8440–8841.
- [50] (a) R.S. Mulliken, *J. Chem. Phys.* 23 (1955) 1833;
(b) R.S. Mulliken, *J. Chem. Phys.* 23 (1955) 1841;
(c) R.S. Mulliken, *J. Chem. Phys.* 23 (1955) 2338;
(d) R.S. Mulliken, *J. Chem. Phys.* 23 (1955) 2343.